FOCUS ISSUE OF SELECTED PRESENTATIONS FROM IMLB 2014

Cycling Performances of Lithium-Air Cells Assembled with Mixed Electrolytes of Ionic Liquid and Diethylene Glycol Diethyl Ether

Sang-Min Han, Jae-Hong Kim, and Dong-Won Kim*,z

Department of Chemical Engineering, Hanyang University, Seungdong-Gu, Seoul 133-791, Korea

Ionic liquid-based electrolytes composed of diethylene glycol diethyl ether (DEGDEE) and 1-butyl-1-methyl pyrrolidinium bis(trifluoromethane) sulfonyl imide (BMP-TFSI) were prepared and evaluated for non-aqueous lithium-air cell applications. Adding an appropriate amount of BMP-TFSI to the electrolyte solution improved ionic conductivity, oxidative stability and interfacial stability, and reduced flammability and volatility. When BMP-TFSI was mixed with DEGDEE under optimal condition, the cycle performance was remarkably improved as compared with either the organic electrolyte or ionic liquid electrolyte alone. The Li-air cell assembled with an optimized ionic liquid-based mixed electrolyte initially delivered a high discharge capacity of 10,620 mAh g^{-1} and exhibited good cycling stability exceeding 150 cycles at a current density of 0.1 mA cm^{-2} by limiting depth of discharge to 500 mAh g^{-1}.

Manuscript submitted October 29, 2014; revised manuscript received December 27, 2014. Published January 8, 2015. This was Paper 519 presented at the Como, Italy, Meeting of the IMLB, June 10–14, 2014. *This paper is part of the Focus Issue of Selected Presentations from IMLB 2014.*

Rechargeable Li-air batteries using oxygen in the air have attracted great interest as a potential power source due to their high theoretical specific energy of 11,000 Wh kg^{-1}, which is close to that of conventional gas-powered engines.[1–8] The non-aqueous Li–air battery usually consists of a lithium negative electrode, an organic electrolyte and a porous carbon positive electrode. The successful development of Li-air batteries depends on these components having long-term stability and highly reversible formation and decomposition of Li_2O_2 as a desired discharge product.[6,9–11] The electrolyte presents one of the greatest challenges to practically exploiting Li–air batteries. Initially, alkyl carbonate-based electrolytes, such as propylene carbonate, were widely studied; however, they are susceptible to nucleophilic attack by oxygen reduction species.[12–14] Ether-based electrolytes, such as tetra(ethylene glycol) dimethyl ether (TEGDME), are known to be more stable than alkyl carbonates.[15–18] Although TEGDME has been identified as a relatively stable electrolyte against nucleophilic attack, the repeated cycling caused irreversible chemical changes in the electrolyte, which resulted in formation of decomposition products such as Li_2CO_3, HCO_2Li, CH_3CO_2Li, CO_2 and H_2O. To overcome the irreversibility caused by attack of superoxide anion radical ($O_2^{\bullet-}$), our group investigated a diethylene glycol diethyl ether (DEGDEE)-based electrolyte. The Li-air cell with a DEGDEE-based electrolyte exhibited a fairly stable cycling behavior when compared with that of a TEGDME-based Li-air cell.[19] Nevertheless, the cycling stability was still not satisfactory due to electrolyte instability caused by its volatile nature and parasitic reactions between the organic electrolyte and the oxygen reduction species. As an alternative electrolyte, ionic liquids can be promising candidate because they have negligible vapor pressure, are non-flammable and have high electrochemical stability.[20–22] Moreover, ionic liquids can effectively interact with superoxide anion radicals and thus mitigate radical attacks during cycling.[23–25] These properties make ionic liquids especially desirable as stable electrolytes for Li-air cells. However, the ionic conductivity of ionic liquid electrolytes is relatively low due to their high viscosity, and the solubility and diffusion coefficient of oxygen in ionic liquid electrolytes are much lower than in organic electrolytes, which prevent their exclusive use in lithium-air cells.

To solve the problems related with the volatility and irreversible decomposition of organic electrolytes as well as the high viscosity of ionic liquid electrolytes, we mixed DEGDEE and ionic liquid electrolyte at different compositions. In our work, 1-butyl-1-methyl pyrrolidinium bis(trifluoromethane) sulfonyl imide (BMP-TFSI) was selected as the ionic liquid, because it can effectively stabilize superoxide anion radicals and has good stability toward lithium metal electrodes.[24–27] With these mixed electrolytes, we assembled the Li-air cells composed of a lithium negative electrode and a carbon positive electrode (without a catalyst), and their cycling performances were evaluated. The Li-air cell assembled with an optimized electrolyte initially delivered a high discharge capacity of 10,620 mAh g^{-1} based on the weight of carbon in the air electrode. By limiting the depth of discharge to 500 mAh g^{-1} and constraining the carbon loading to 1.0 mg cm^{-2}, the cell exhibited good cycling stability exceeding 150 cycles at a current density of 0.1 mA cm^{-2}. To the best of our knowledge, this report is the first to demonstrate the cycling performance of lithium-air cells with mixed DEGDEE and BMP-TFSI electrolytes.

Experimental

Electrolyte preparation.— BMP-TFSI was purchased from Chem Tech Research Incorporation and used after drying under a vacuum at 100°C for 24 h. The water content in BMP-TFSI after drying was determined to be less than 20 ppm by Karl Fisher titration using a Mettler-Toledo Coulometer. The ionic conductivity of BMP-TFSI was 2.4 mS cm^{-1} at room temperature. DEGDEE was anhydrous grade purity purchased from Sigma Aldrich and was used after drying with pre-dried 4A molecular sieve for several days. The mixed electrolyte was prepared by adding predetermined amounts of lithium bis(trifluoromethane) sulfonyl imide (LiTFSI, Sigma Aldrich) to the mixed solution of DEGDEE and BMP-TFSI in a glove box filled with purified argon. The contents of ionic liquid in the mixed solutions were 0, 25, 50, 75 and 100% based on volume. The electrolyte systems will be presented as IL N, where N is the volumetric% of ionic liquid in the mixed solutions.

Cell assembly.— The carbon-based air electrode was prepared by coating an N-methyl pyrrolidone (NMP)-based slurry containing Ketjen black EC300JD and poly(vinylidiene fluoride) (PVDF) binder (8:2 by weight) on a gas diffusion layer (SGL GROUP, Germany). The electrode was dried in a vacuum oven for 12 h at 100°C to remove the residual NMP. The area of the carbon air electrode was 1.13 cm^2, and the carbon loading in the air electrode was about 1.0 mg cm^{-2}.

*Electrochemical Society Active Member.
zE-mail: dongwonkim@hanyang.ac.kr

The negative electrode consisted of lithium metal (Honjo Metal Co. Ltd., 100 μm) that was pressed on a copper current collector. The lithium-air cell comprising a lithium electrode, glass microfiber filter paper (Whatman grade GF/D) and a carbon air electrode was assembled with a mixed electrolyte into a custom-designed Swagelok-type cell fabricated from Teflon, as previously reported.[19] All cells were assembled in an argon-filled glove box where the H_2O and O_2 contents were kept below 1 ppm.

Measurements.— The viscosity measurements of the mixed electrolytes were performed with a viscometer (Schott AVS 350). The ionic conductivity of the mixed electrolyte was measured with a Cond 3210 conductivity meter (WTW GmbH, Germany) at 25°C. The lithium transference number was measured at 25°C by a combination of AC impedance and DC polarization methods.[28] AC impedance measurements were performed to measure interfacial resistances using an impedance analyzer over a frequency range of 1 mHz to 100 kHz with an amplitude of 10 mV. The self-extinguishing time (SET) was measured to quantify the flammability of the electrolyte, as previously described.[29] Briefly, the SET value was obtained by igniting pre-weighed electrolyte solution soaked in an inert glass-fiber wick (3 cm × 3 cm), followed by measuring the time required for the flame to be extinguished. The measurements were repeated at least five times to get reproducible SET values. The electrochemical stability of the mixed electrolyte was determined with linear sweep voltammetry (LSV) measured on a platinum working electrode with lithium metal counter and reference electrodes at a scanning rate of 1.0 m V s^{-1}. For the cycling tests, the cell was placed in a chamber filled with high-purity oxygen gas at a slightly higher than 1.0 atm. Charge and discharge cycling tests of the lithium-air cells were performed with battery testing equipment (WBCS 3000, Wonatech) in open conditions at 25°C. Charge and discharge curves were recorded galvanostatically at a constant current rate of 100 mA (g carbon)$^{-1}$ within a limited capacity of 1,000 mAh g^{-1} in the voltage range of 2.0 to 5.0 V, unless specified otherwise. We considered the mass of Ketjen black as the active material loading in the air electrode.

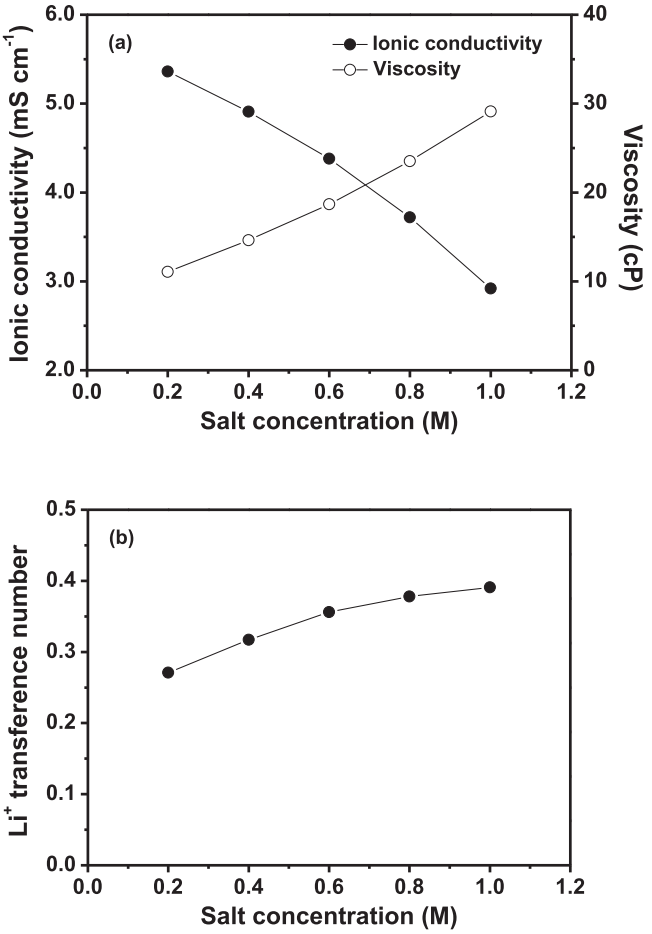

Figure 1. (a) Ionic conductivity and viscosity, and (b) lithium transference number as a function of salt concentration in the mixed electrolyte (IL 50) at 25°C.

Results and Discussion

Physical properties of the DEGDEE and BMP-TFSI used to prepare the mixed electrolytes are summarized in Table I. As shown in Table I, DEGDEE had a glyme structure like other ether-based solvents. Its low viscosity makes the electrolyte dissolving 1.0 M LiTFSI have fairly high ionic conductivity (4.7×10^{-3} S cm^{-1}) at 25°C. However, the volatile characteristics of DEGDEE at room temperature may cause gradual vaporization of the solvent in Li-air cells operated in open conditions. On the other hand, the vapor pressure of BMP-TFSI was negligible at room temperature. Moreover, alkyl groups bounded to the N atoms are very poor leaving groups, which makes it less prone to $O_2^{\bullet-}$ attack. However, it had a lower ionic conductivity and higher viscosity than did the DEGDEE-based electrolyte, which may retard oxygen and Li^+ ion transport in the electrolyte. To overcome the drawbacks of each electrolyte system, we prepared mixed electrolytes containing DEGDEE and BMP-TFSI at different ratios.

To optimize the salt concentration of the mixed electrolytes, we investigated the effect of the salt concentration on ionic conductivity and viscosity of a mixed electrolyte containing 50/50 DEGDEE/BMP-TFSI, and the results are given in Figure 1a. Unlike conventional organic electrolytes, the ionic conductivity continuously decreased with increasing salt concentrations from 0.2 to 1.0 M, because the decrease of ionic mobility due to the increased viscosity surpasses the increase in number of free ions arising from the dissociation of the salt. This result suggests that the salt concentration should be kept low to achieve high ionic conductivity in mixed electrolytes with highly viscous ionic liquid. It is noticeable that the ions in BMP-TFSI do not participate in the electrochemical reaction in the lithium-air cells. Thus the lithium transference number was measured to examine the contribution of lithium ion conductivity in the mixed electrolyte. As shown in Figure 1b, the lithium transference number was gradually

Table I. Molecular structures and physical properties of DEGDEE and BMP-TFSI, and ionic conductivities of 1.0 M LiTFSI electrolytes at 25°C (black: carbon atom, red: oxygen atom, blue: nitrogen atom, yellow: sulfur atom, purple: fluorine atom).

	Molecular structure	Boiling point (°C)	Vapor pressure (mm Hg)	Viscosity (cP)	Conductivity (mS cm^{-1})
DEGDEE	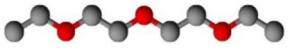	186	0.5	1.4	4.7
BMP-TFSI	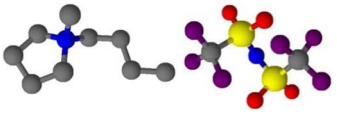	–	1.0×10^{-7}	84.0	0.9

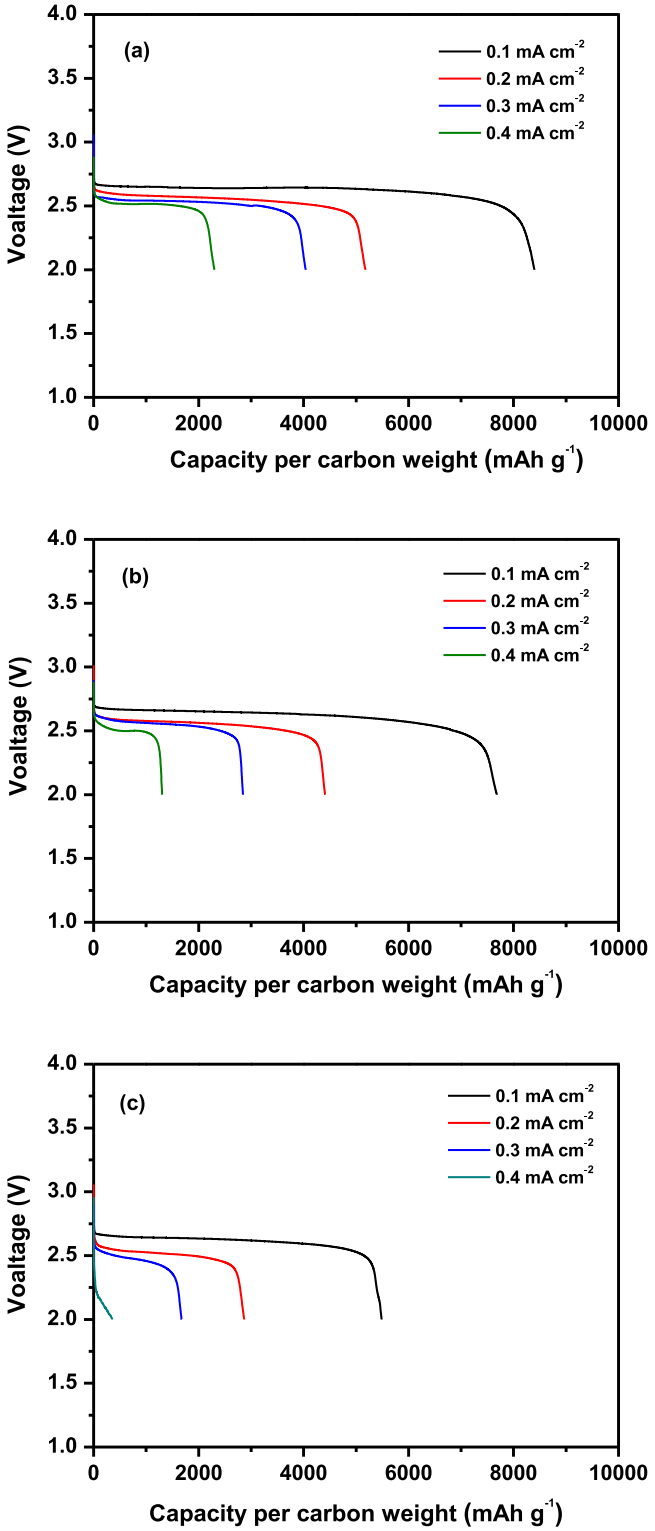

Figure 2. Initial discharge curves of lithium-air cells assembled with mixed electrolyte (IL 50) of different salt concentrations under different current densities. (a) 0.2 M, (b) 0.6 M and (c) 1.0 M.

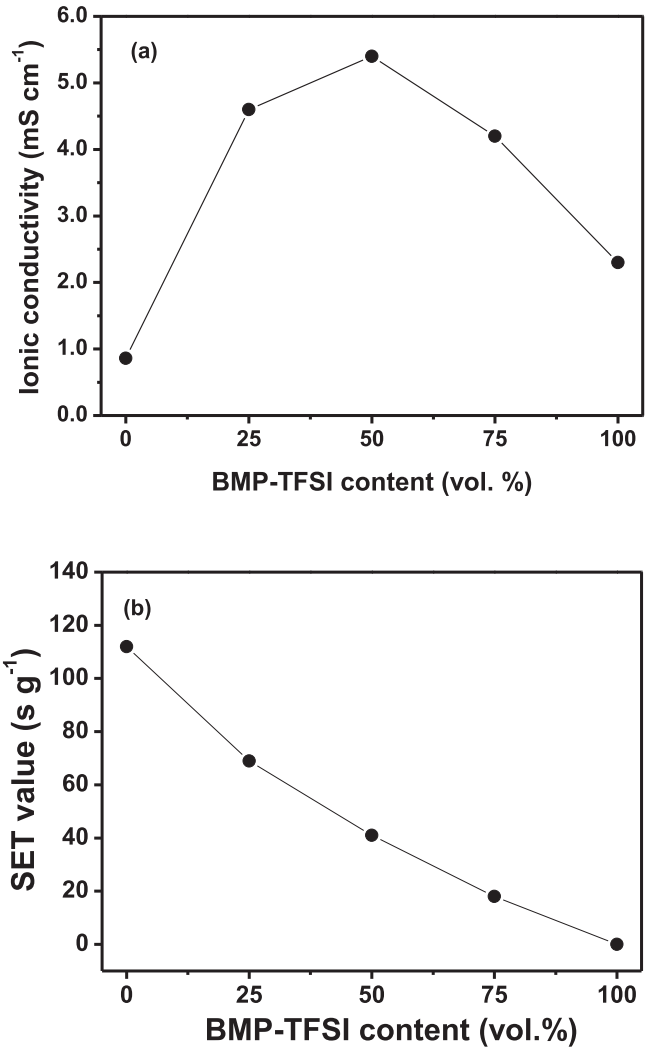

Figure 3. (a) Ionic conductivity and (b) SET values of mixed electrolytes as a function of BPM-TFSI content. (Salt concentration was 0.2 M).

increased with salt concentration. This result can be ascribed to the increase in number of lithium ions with increasing Li salt concentration. Lithium ion conductivity (σ_{Li+}) estimated from ionic conductivity and lithium transference number was the highest at 0.6 M.

The effect of salt concentration on rate capability of the cell was investigated in the mixed electrolyte, IL 50. After cell assembly, the cells were fully discharged to a cut-off voltage of 2.0 V at different current densities ranging from 0.1 to 0.4 mA cm^{-2}. It should be noted that the cell using only gas diffusion layer delivered a limited discharge capacity of 50.1 mAh g^{-1} at a current density of 0.1 mA cm^{-2}, which was quite lower than the discharge capacity (8397.4 mAh g^{-1}) obtained in the cell with Ketjen Black carbon. Thus, it is safe to report the discharge capacity of the lithium-air cell based on the weight of Ketjen Black carbon. As shown in Figure 2, the overpotential was increased with increasing current density, which resulted in decrease of discharge capacity. Among the cells investigated, the cell assembled with mixed electrolyte containing 0.2 M LiTFSI exhibited higher discharge capacities than other cells with different salt concentrations for all current densities, though the mixed electrolyte with 0.6 M salt had the highest lithium ion conductivity. This result implies that the kinetics of oxygen reduction reaction is affected by oxygen diffusion rate as well as lithium ion conduction. Accordingly, the 0.2 M solution provided the best rate performance due to its lowest viscosity and relatively high Li^+ conductivity. Based on above results, 0.2 M salt was used in all further experiments.

The ionic conductivities of the mixed electrolytes with different compositions are shown in Figure 3a. The ionic conductivity initially increased with increasing BMP-TFSI content, reaching a maximum (5.4×10^{-3} S cm^{-1}) at 50% by volume. Because BMP-TFSI itself has a lot of cations and anions, the number of ions in the electrolyte solution increased with increasing BMP-TFSI content. As a result,

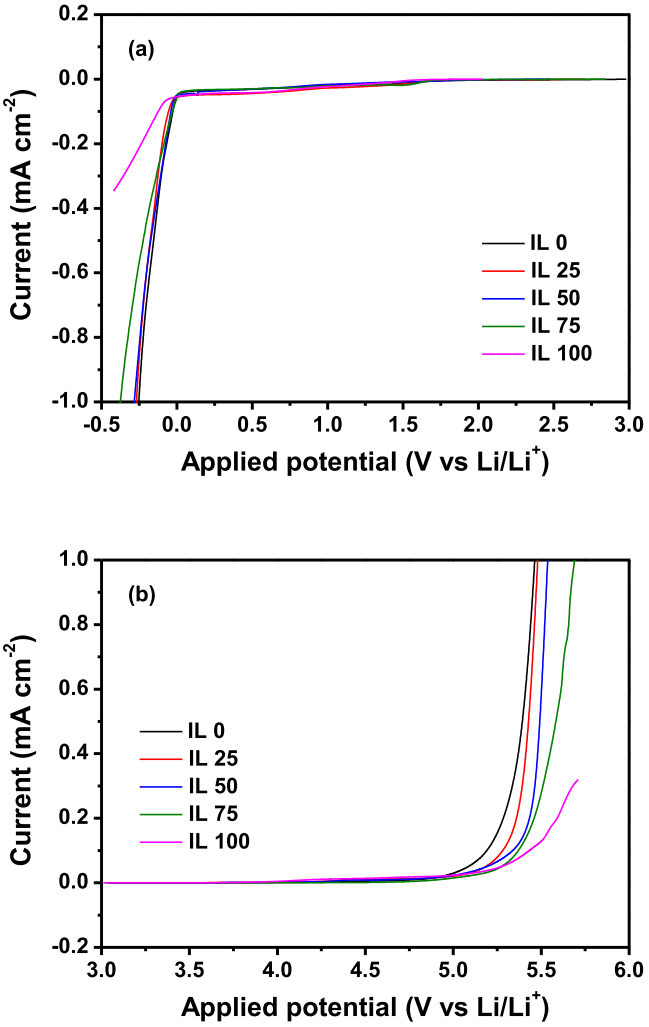

Figure 4. Linear sweep voltammograms of mixed electrolytes without oxygen: (a) cathodic scan and (b) anodic scan (scan rate: 1 mV s^{-1}). (Temperature: 25°C).

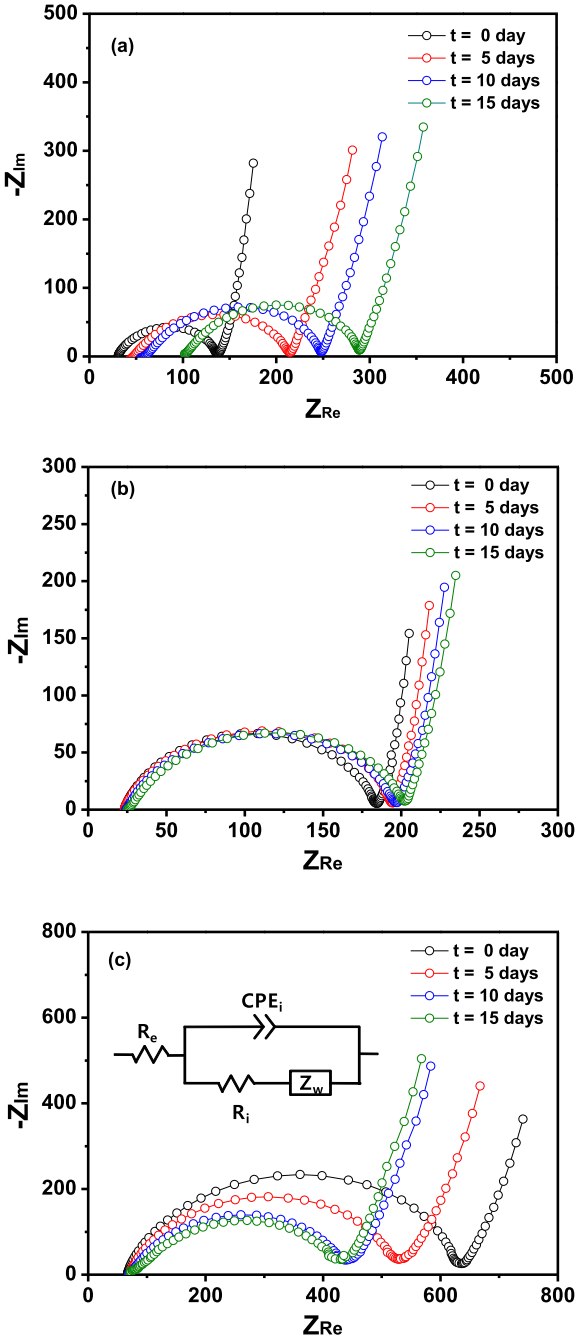

Figure 5. AC impedance spectra of lithium-air cells at open circuit potential as a function of storage time at 25°C. The cells were assembled with (a) IL 0, (b) IL 50, and (c) IL 100.

the ionic conductivity initially increased with the BMP-TFSI content. Adding BMP-TFSI, however, increased the viscosity of the mixed electrolyte due to the increased ion-solvent interactions and coulombic interactions between ionic species in the mixed electrolytes. Thus, a decrease in ionic conductivity at BMP-TFSI contents beyond 50 vol% was attributed to the increased viscosity. SET values were measured to compare the flammable behavior of the mixed electrolyte with varying BMP-TFSI content, and the results are shown in Figure 3b. BMP-TFSI did not combust, even during ignition with a flame source (i.e., its SET value is 0 s g^{-1}). As BMP-TFSI was added to the organic electrolyte, both the SET value and flame intensity decreased; hence, the flammability dropped as shown in figure. This result suggests that adding an ionic liquid-based electrolyte to the electrolyte solution reduces the flammability of the electrolyte, enhancing the safety of Li-air cells.

Linear sweep voltammetry curves of the mixed electrolytes in the absence of oxygen are shown in Figure 4. In the cathodic scan shown in Figure 4a, large reductive currents were observed around 0 V vs. Li/Li$^+$ for all electrolyte systems, which correspond to the reductive deposition of lithium onto the electrode (i.e., $Li^+ + e \rightarrow Li$). A decrease of reduction potential for lithium deposition in the pure ionic liquid electrolyte (i.e., IL 100) was associated with an increased ionic resistance. The absence of significant reduction peaks before lithium plating indicates that the mixed electrolytes were reductively stable up to 0 V vs. Li/Li$^+$. In the anodic scan shown in Figure 4b, the anodic current starts to increase at around 5.0 V vs. Li/Li$^+$ in the DEGDEE-based electrolyte (i.e., IL 0), which can be attributed to the oxidative decomposition of the electrolyte. The decomposition potential increases slightly with increasing BMP-TFSI content in the mixed electrolytes, which demonstrates that adding BMP-TFSI to the organic electrolyte increase the anodic stability of the electrolyte.

We obtained AC impedance spectra of cells at open circuit potential as a function of storage time to understand the dynamic behavior of Li-air cells exposed to open oxygen atmosphere, and the results are shown in Figure 5. According to previous report in lithium-air cells,[30] a simple equivalent circuit to describe the observed impedance spectra at the early stages of cycling is shown in inset of Figure 5c. In this equivalent circuit, R_e is the electrolyte resistance and corresponds to

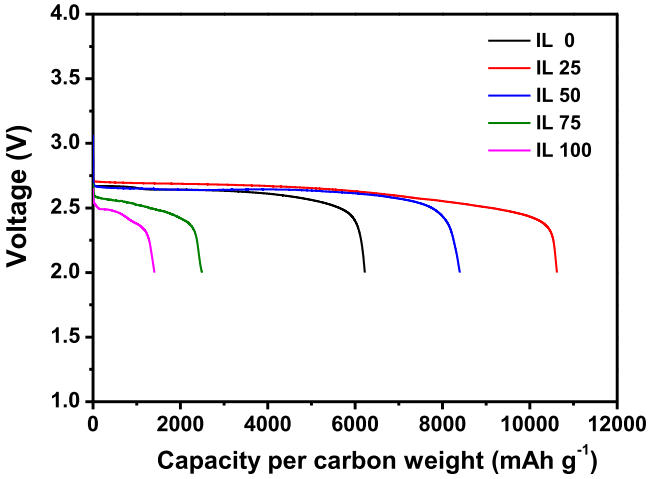

Figure 6. Initial discharge curves of lithium-air cells assembled with different electrolyte systems. The cells were fully discharged to 2.0 V at a constant current density of 0.1 mA cm^{-2} (100 mA g^{-1}).

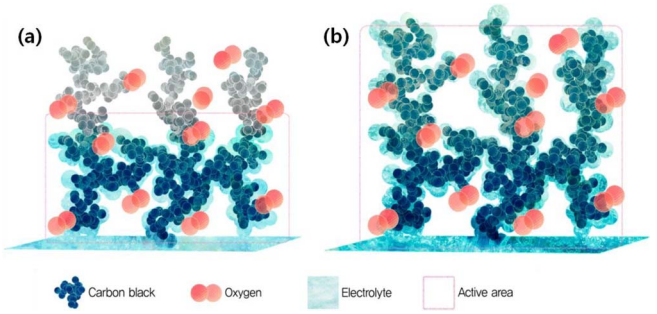

Figure 7. Schematic illustration of the wettability of porous carbon electrode in lithium-air cells assembled with different electrolytes. (a) IL 0 and (b) IL 100.

the high frequency intercept at the real axis. R_i is the interfacial (charge transfer) resistance at two electrodes and CPE_i (constant phase element) denotes the capacitive contributions of the electrodes to reflect the depressed semicircular shape. In the organic electrolyte-based cell (IL 0), the initial overall resistance (137.0 Ω), including R_e and R_i, was lower than in any other cells. However, both the electrolyte resistance and interfacial resistance increased significantly with time. After 15 days, the electrolyte resistance was remarkably increased from 30.9 to 102.2 Ω, and the interfacial resistance was increased from 106.1 to 187.0 Ω. This result indicates that the organic solvent in the cell continuously evaporated, and the loss of organic solvent hindered the charge transfer reaction at the air electrode/O_2/electrolyte interface. On the other hand, the electrolyte resistance in the cell with pure ionic liquid electrolyte (IL 100) was almost unchanged even though its initial value was high (67.3 Ω), as shown in Figure 5c, indicating that the ionic electrolyte was not lost even in open atmosphere conditions. It is noticeable that the interfacial resistance of the cell decreased gradually and eventually stabilized. The initial decrease in interfacial resistance was likely due to continuous penetration of the highly viscous ionic liquid electrolyte into the porous carbon electrode, which gradually increased participation of the active material in the charge transfer reaction. However, the overall resistance of the cell (429.8 Ω) after 15 days was relatively high due to the highly viscous nature of the ionic liquid electrolyte. When DEGDEE and BMP-TFSI were mixed at volume ratio of 50/50, both the electrolyte resistance and the interfacial resistance decreased as compared to those of ionic liquid-based cell. Interestingly, both R_e and R_i were almost constant to be 25.4 Ω and 176.7 Ω through times investigated, respectively (Figure 5b). These results suggest that adding an ionic liquid to an organic electrolyte is an effective way to suppress evaporation of the organic solvent and stabilize the interfacial resistance at the air electrode/O_2/electrolyte interface.

The full discharge capacities of the Li-air cells were measured at a constant current density of 0.1 mA cm^{-2} (100 mA g^{-1}). Figure 6 shows the first full discharge curves of cells assembled with different electrolytes. The cell with IL 25 had the lowest overpotential and delivered the highest discharge capacity (10,620 mAh g^{-1}, specific capacity is defined per gram of Ketjen Black carbon) among the cells examined. Adding more than 25 vol% BMP-TFSI adversely affected the initial discharge capacity. This result can be ascribed to the combined effects of the high ionic conductivity of DEGDEE and the wettability and stability of BMP-TFSI in the mixed electrolyte. As the BMP-TFSI content increased, the mixed electrolyte became hydrophobic, allowing it to effectively wet the hydrophobic carbon electrodes, as illustrated in Figure 7. However, adding further ionic liquid decreased the initial discharge capacity of the cell due to the increased viscosity. These results imply that optimizing the electrolyte composition is important for achieving good cycling performance.

Figure 8 shows the discharge and charge curves of lithium-air cells assembled with different electrolytes, which were obtained by controlling the depth of discharge to 1,000 mAh g^{-1} at a constant current density of 0.1 mA cm^{-2} (100 mA g^{-1}). It is clearly seen that the polarization for the charge and discharge cycles increased with cycle number. Among the cells investigated, the cell assembled with IL 25 had the best cycling stability. In this cell, reversible charge and discharge cycling was observed for up to the 65th cycles. In cells with more than 25 vol% BMP-TFSI, the gap between the charge and discharge profiles became more significant during earlier cycles, which can be ascribed to the slow kinetics of the oxygen reduction and oxygen evolution reactions at the carbon electrode due to the high viscosity of the electrolyte solution. Interestingly, the cell assembled with 25 vol% BMP-TFSI retained capacity better than the organic electrolyte-based cell. As reported previously, the pyrrolidinium cation in BMP-TFSI has a weak acidity and thus effectively neutralizes the weakly basic $O_2^{\bullet-}$.[25] These interactions protect the electrolyte solution from superoxide radical attack and improves the cycle life compared with the organic electrolyte alone. The oxygen reduction and evolution reaction mechanism in BMP-TFSI has been reported by Abraham et al.[21,24] According to their reports, Li_2O_2 was formed not from electrochemical reaction of LiO_2 but from the chemical decomposition reaction, which could be explained by the hard soft acid base (HSAB) theory of Pearson.[31] Since Li^+ is a hard Lewis acid in ionic liquid, while O_2^- and O_2^{2-} are soft and hard Lewis base, respectively, the chemical decomposition of the unstable LiO_2 to form Li_2O_2 is favorable.[24] The suppressed solvent evaporation when BMP-TFSI is added can be attributed the stable cycling behavior of the cell with 25 vol% ionic liquid. These results indicate that mixing an ionic liquid with organic solvent under optimal condition remarkably improves the cycle life of a Li-air cell compared with either the organic electrolyte or ionic liquid electrolyte alone. Each component seems to compensate for the drawbacks of the other, thus bringing synergistic effects to the cell performance.

The buildup of insoluble discharge products in the discharged cell may inhibit the transport of lithium ions, oxygen and electrons to the electrochemical interface, which may permanently choke a porous carbon electrode after a few cycles.[32,33] To prevent insulating discharge products from accumulating, the capacity utilization was limited to 500 mAh g^{-1}. The cell was cycled at a constant current density of 0.1 mA cm^{-2} (100 mA g^{-1}), which corresponds to 0.2C rate. Figure 9a, 9b, and 9c show the charge and discharge profiles of a lithium-air cell assembled with IL 25 as a function of the cycle number. The cell had good charge-discharge cycling stability with a coulombic efficiency of 100% through 150 cycles, as depicted in Figure 9d. When the depth of discharge is limited to 500 mAh g^{-1}, the amount of discharge products deposited on the surface of the carbon electrode decreases, which may suppress choking of the carbon electrode and

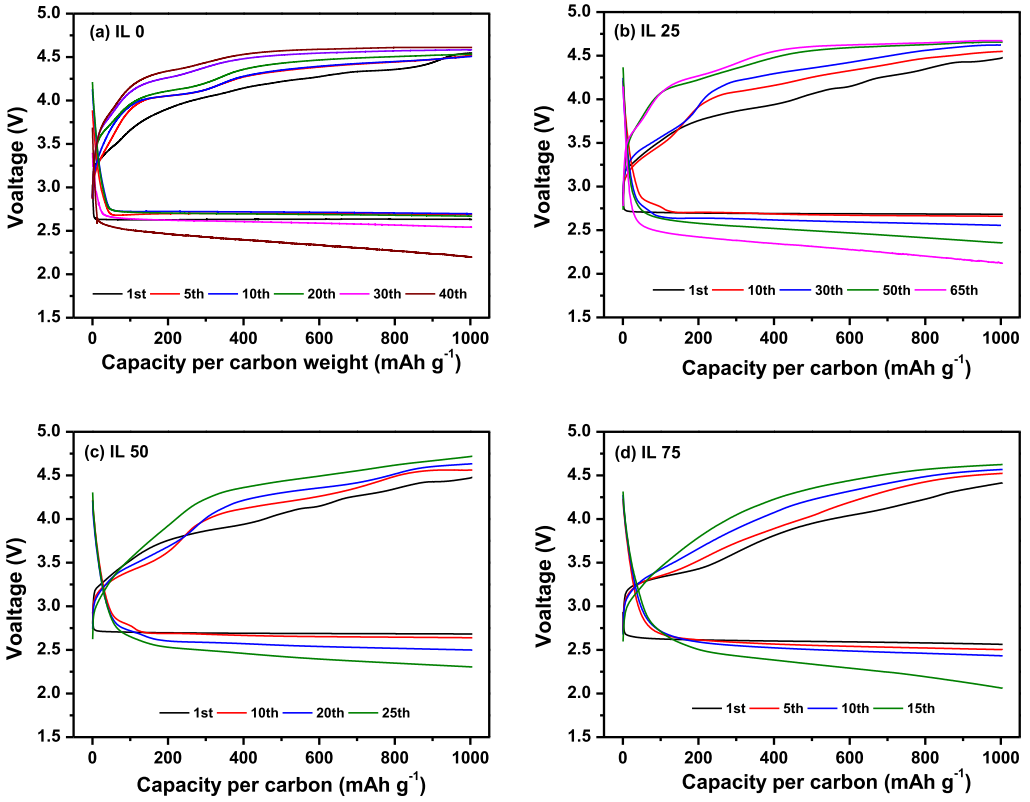

Figure 8. Discharge and charge curves of lithium-air cells assembled with different electrolytes at a constant current density of 0.1 mA cm^{-2} (100 mA g^{-1}), where the carbon loading in the air cathode was 1.0 mg cm^{-2}: (a) IL 0, (b) IL 25, (c) IL 50 and (d) IL 75.

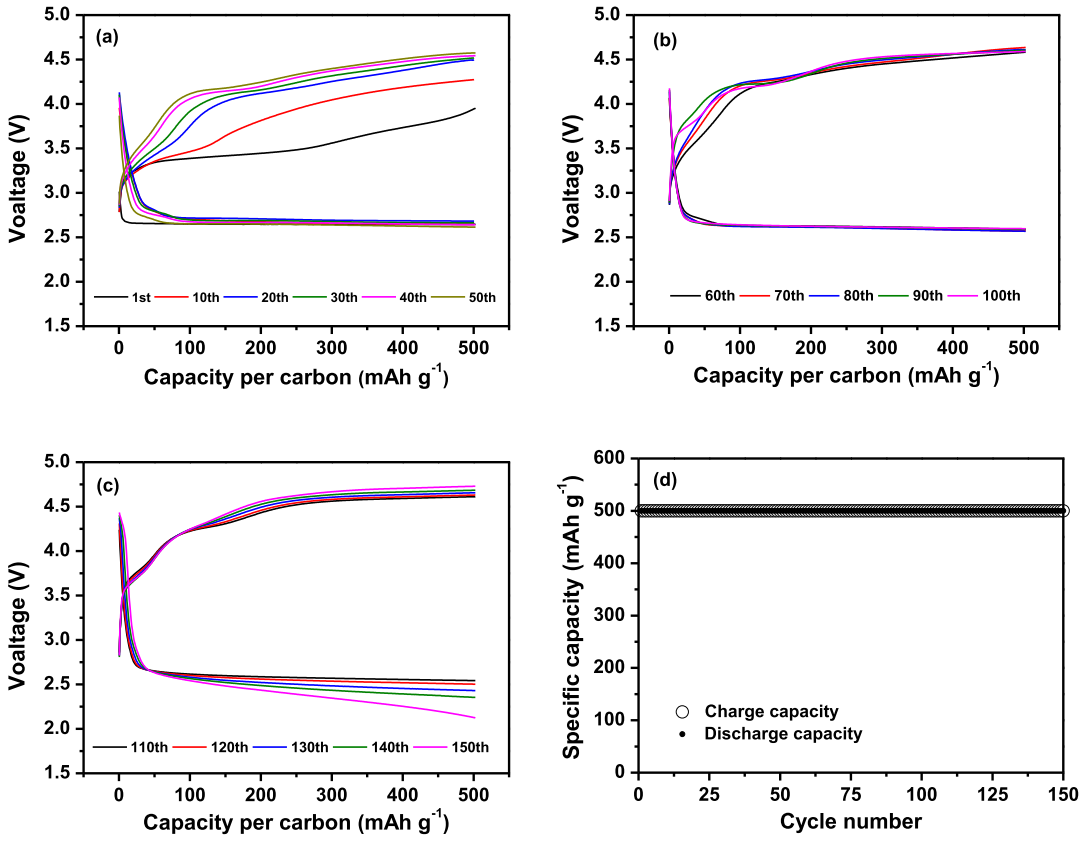

Figure 9. (a)-(c) Discharge and charge curves of the lithium-air cell assembled with IL 25 at a constant current density of 0.1 mA cm^{-2} (100 mA g^{-1}), when the capacity utilization was limited to 500 mAh g^{-1}. (d) Discharge and charge capacities as a function of the cycle number. The carbon loading in the air cathode was 1.0 mg cm^{-2}.

also reduce electrode polarization. Also, the transport of oxygen into the interior of the carbon electrode can be facilitated. To the best of our knowledge, the cycling stability of the Li-air cell in this study is superior to other reports based on ionic liquid electrolyte[34,35] or its mixture with organic solvents.[25,26,36] More systematic studies on characteristics of the air electrode, such as porosity, type of binder, electrode composition and catalyst, are currently in progress to further improve the cycling performance of lithium-air cells with ionic liquid-based electrolytes.

Conclusions

We investigated ionic liquid-based electrolytes composed of DEGDEE and BMP-TFSI for use in lithium-air cells. Adding a proper amount of BMP-TFSI to DEGDEE-based organic electrolytes improved the ionic conductivity, oxidative stability and long-term stability by suppressing the evaporation of the organic solvent. When BMP-TFSI was mixed with DEGDEE under optimal conditions, the cycle life of the Li-air cell was remarkably improved compared with either the organic electrolyte or ionic liquid electrolyte alone. The Li-air cell assembled with an optimized electrolyte initially delivered a high discharge capacity and was stable for more than 150 cycles at a current density of 0.1 mA/cm^2.

Acknowledgments

This work was supported by the Energy Efficiency & Resources Core Technology Program (No. 20112010100110/KIER B4-2462) and Human Resources Development Program (No. 20124010203290) of the Korea Institute of Energy Technology Evaluation and Planning (KETEP) grant funded by the Korea government Ministry of Trade, Industry and Energy.

References

1. K. M. Abraham and Z. Jiang, *J. Electrochem. Soc.*, **143**, 1 (1996).
2. J. P. Zheng, R. Y. Liang, M. Hendrickson, and E. J. Plichta, *J. Electrochem. Soc.*, **155**, A432 (2008).
3. G. Girishkumar, B. McCloskey, A. C. Luntz, S. Swanson, and W. J. Wilcke, *J. Phys. Chem. Lett.*, **1**, 2193 (2010).
4. A. Kraytsberg and Y. Ein-Eli, *J. Power Sources*, **196**, 886 (2011).
5. J. Christensen, P. Albertus, R. S. Sanchez-Carrera, T. Lohmann, B. Kozinsky, R. Liedtke, J. Ahmed, and A. Kojica, *J. Electrochem. Soc.*, **159**, R1 (2012).
6. P. G. Bruce, S. A. Freunberger, L. J. Hardwick, and J.-M. Tarascon, *Nature Mater.*, **11**, 19 (2012).
7. F. Cheng and J. Chen, *Chem. Soc. Rev.*, **41**, 2172 (2012).
8. R. Black, B. Adams, and L. F. Nazar, *Adv. Energy Mater.*, **2**, 801 (2012).
9. Y. Shao, F. Ding, J. Xiao, J. Zhang, W. Xu, S. Park, J.-G. Zhang, Y. Wang, and J. Liu, *Adv. Funct. Mater.*, **23**, 987 (2013).
10. V. S. Bryantsev, J. Uddin, V. Giordani, W. Walker, D. Addison, and G. V. Chase, *J. Electrochem. Soc.*, **160**, A160 (2013).
11. M. Balaish, A. Kraytsberg, and Y. Ein-Eli, *Phys.Chem.Chm.Phys.*, **16**, 2801 (2014).
12. S. A. Freunberger, Y. H. Chen, Z. Q. Peng, J. M. Griffin, L. J. Hardwick, F. Barde, P. Novak, and P. G. Bruce, *J. Am. Chem. Soc.*, **133**, 8040 (2011).
13. G. M. Veith, N. J. Dudney, J. Howe, and J. Nanda, *J. Phys. Chem. C*, **115**, 14325 (2011).
14. J. Xiao, J. Hu, D. Wang, D. Hu, W. Xu, G. L. Graff, Z. Nie, J. Liu, and J. G. Zhang, *J. Power Sources*, **196**, 5674 (2011).
15. B. D. McCloskey, D. S. Bethune, R. M. Shelby, G. Girishkumar, and A. C. Luntz, *J. Phys. Chem. Lett.*, **2**, 1161 (2011).
16. J. R. Harding, Y.-C. Lu, Y. Tsukada, and Y. Shao-Horn, *Phys. Chem. Chem. Phys.*, **14**, 10540 (2012).
17. G. M. Veith, J. Nanda, L. H. Delmau, and N. J. Dudney, *J. Phys. Chem. Lett.*, **3**, 1242 (2012).
18. H.-G. Jung, J. Hassoun, J.-B. Park, Y.-K. Sun, and B. Scrosati, *Nature Chem.*, **4**, 579 (2012).
19. S. M. Han, J. H. Kim, and D. W. Kim, *J. Electrochem. Soc.*, **161**, A856 (2014).
20. J. Fuller, R. T. Carlin, R. A. Osteryoung, P. Koranaios, and R. Mantz, *J. Electrochem. Soc.*, **145**, 24 (1998).
21. C. J. Allen, S. Mukerjee, E. J. Plichta, M. A. Hendrickson, and K. M. Abraham, *J. Phys. Chem. Lett.*, **2**, 2420 (2011).
22. M. Kar, T. J. Simons, M. Forsyth, and D. R. MacFarlane, *Phys. Chem. Chem. Phys.*, **16**, 18658 (2014).
23. F. De Giorgio, F. Soavi, and M. Mastragostino, *Electrochem. Commun.*, **13**, 1090 (2011).
24. C. J. Allen, J. Hwang, R. Kautz, S. Mukerjee, E. J. Plichta, M. A. Hendrickson, and K. M. Abraham, *J. Phys. Chem. C*, **116**, 20755 (2012).
25. B. G. Kim, J. N. Lee, D. J. Lee, J. K. Park, and J. W. Choi, *ChemSusChem*, **6**, 443 (2013).
26. L. Cecchetto, M. Salomon, B. Scrosati, and F. Croce, *J. Power Sources*, **213**, 233 (2012).
27. J. Zheng, M. Gu, H. Chen, P. Meduri, M. H. Engelhard, J.-G. Zhang, J. Liu, and J. Xiao, *J. Mater. Chem. A*, **1**, 8464 (2013).
28. J. Evance, C. A. Vincent, and P. G. Bruce, *Polymer*, **28**, 2324 (1987).
29. K. Xu, M. S. Ding, S. Zhang, J. L. Allen, and T. R. Jow, *J. Electrochem. Soc.*, **149**, A622 (2002).
30. C. O'Laoire, S. Mukerjee, E. J. Plichta, M. A. Hendrickson, and K. M. Abraham, *J. Electrochem. Soc.*, **158**, A302 (2011).
31. R. G. Pearson, *J. Am. Chem. Soc.*, **85**, 3533 (1963).
32. T. Ogasawara, A. Debart, M. Holzapfel, P. Novak, and P. G. Bruce, *J. Am. Chem. Soc.*, **128**, 1390 (2006).
33. M. J. Trahan, S. Mukerjee, E. J. Plichta, M. A. Hendrickson, and K. M. Abraham, *J. Electrochem. Soc.*, **160**, A259 (2013).
34. H. Nakamoto, Y. Suzuki, T. Shiotsuki, F. Mizuno, S. Higashi, K. Takechi, T. Asaoka, H. Nishikoori, and H. Iba, *J. Power Sources*, **243**, 19 (2013).
35. T. Kuboki, T. Okuyama, T. Ohsaki, and N. Takami, *J. Power Sources*, **146**, 766 (2005).
36. K. Cai, H. Jiang, and W. Pu, *Int. J. Electrochem. Sci.*, **9**, 390 (2014).